Advantages and Problems of Nanocrystalline Scintillators

N. V. Klassen, V. V. Kedrov, V. N. Kurlov, Yu A. Ossipyan, S. Z. Shmurak, I. M. Shmyt'ko, G. K. Strukova, N. P. Kobelev, E. A. Kudrenko, O. A. Krivko, A. P. Kiselev, A. V. Bazhenov, and T. N. Fursova

***Abstract*—Our experiments with nanocrystalline scintillating rare earth oxides and rare earth fluorides have shown that in some cases nanoscopic dimensions provide essential improvement of the most important scintillation parameters: light yield, kinetics of scintillations, radiation hardness, etc. We found that in the range from 20 to 100-nm of the oxide and fluoride particles there are 3 types of layered structures: with expanded exterior layer, with changed phase structure, and with changed chemical composition. These layered structures can strongly influence scintillation parameters: cause an increase or decrease in the light yield, vary scintillation kinetics, modify radiation hardness, etc. Control of dimensions and structures of nanoscintillators can be used for significant modifications of parameters of radiation detectors (radical acceleration of kinetics, enhancement of light yield, increase in radiation hardness, etc.). Radiation detectors based on nanoscintillators have promising prospects for applications in new generations of devices for medical diagnostics, security inspection, radiation monitoring of nuclear reactors.**

***Index Terms*—Annealing, luminescence, lutetium compounds, medical imaging, radiation effects, radiation monitoring of nuclear reactors, scintillation detectors, security control.**

I. Introduction

THE search for new effective scintillators with high density, better effectiveness of the ionizing radiation energy conversion to the emitted light, faster kinetics of scintillations and high radiation hardness has been progressed for more than 50 years. The need for new scintillators with essentially improved technical parameters is determined by expanding applications of ionizing radiation scintillation detectors in medical diagnostics devices, antiterrorist inspection systems, control of nuclear power plants, etc. However, in spite of a great number of highly qualified laboratories all over the world involved in this problem, the progress is rather slow. For example, since the mid 20-th century the energy conversion coefficient has improved by only about factor of 1.5 (from 15% in sodium iodide to about 23% in lanthanum bromide and lutetium iodide). These parameters were achieved using bulk single crystals. It was traditionally accepted that to achieve better properties one should prepare bigger crystals with better atomic structure and higher chemical purity doped with effective activators of light emission. However, during the last decade it has become doubtful whether the only way to achieve better scintillation properties is in use of the high quality single crystals, because development of nanoscopic light emitters progresses fast. E.g., manifold increase in light emission efficiency of the semiconductor nanostructures (in comparison with bulk crystals) has been confirmed by a wide spectrum of experiments (see, for example, [1]). The effectiveness of conversion of the energy injected to these structures to the light emission varies from 50% to 80% for various nanosystems. These high conversion coefficients are usually attributed to two mechanisms:a) quantum confinement of electron and phonon states by nanoscopic dimensions of the emitters, which brings to increasing probability of radiative recombination of electron—hole pairs and, on the contrary, to decreasing probability of their non-radiative recombination ;b) arrangement of nanoresonators for virtual photons, increasing their density and thus resulting in enhancement of the probability of spontaneous light emission.These considerations about enhancement of the light emission can be applied to scintillators, because the light emission processes in semiconductors and scintillators are similar, the main difference between them is in the energy pumping methods (electrical or optical pumping in semiconductors and ionizing radiation pumping in scintillators). The ideas of quantum confinement of electron and phonon states, as well as the idea of nanoresonators, which increase density of virtual photons, can be applied directly to nanoscintillators by analogy with semiconductors.The argumentation presented above induced our search for new ways of essential improvement of the scintillation parameters in the direction of development of the nanocrystalline scintillators. The first results obtained in the experiments with complex oxide scintillators turned out to be rather encouraging. E.g., the dependence of light emission intensity on nanograin sizes in yttrium-aluminum garnet with europium activator demonstrated a distinct maximum for about 90-nm diameters and this maximum is by about 4 times higher than effectiveness of the single crystals with the same chemical compositions [2]. In the same paper we described significant improvement of scintillation kinetics in lutetium and gadolinium borates synthesized in our Institute and measured by Prof. S. Derenzo with colleagues from Lawrence Berkeley National Laboratory (USA, California).The most impressive result is manifold decrease in the scintillation rise time (it became less than 0.1 ns). Both experimental results were obtained for nanograins with mean sizes of 70–100 nm. They are much greater than typical dimensions for quantum confinement (usually effects of quantum confinement are observed for less than 10-nm dimensions). But on the other hand, the so called "weak confinement" regime is known [3], when radius of a

Manuscript received June 29, 2007; revised March 21, 2008.

The authors are with the Institute of Solid State Physics, Russian Academy of Sciences, Chernogolovka, Moscow Region 142432, Russia (e-mail: klassen@issp.ac.ru).

Digital Object Identifier 10.1109/TNS.2008.924050

nanoparticle is several times greater than the Bohr exciton radius, nevertheless significant enhancement of the exciton oscillator strength can appear due to "Rashba effect" [4]. In this case the electron excitation polarizes the material of the nanoparticle, where it is confined. This polarization raises additional electric field, which increases the field of electromagnetic wave. The increase in the effective field results in enhancement of oscillator strengths of optical transitions and corresponding rise of light emission.Additional experimental results and considerations presented below show that the nanocrystalline scintillators have complicated layered structures. Anomalies of structural behavior of the nanocrystalline scintillators induce modifications in the conception of their scintillation performance and open new opportunities for significant improvement of exploitation characteristics of the radiation detectors including their sensitivity, spatial and temporal resolutions, radiation hardness.

II. Experimental Procedures

In our experiments we used nanocrystalline oxides (either simple or complex like lutetium borate-$LuBO_3$) of rare earth metals as well as nanocrystalline lutetium and lanthanum fluorides. All the materials were prepared by means of pyrolysis of solutions of initial constituents (e.g., Lu_2O_3 and B_2O_3 for lutetium borate) in melts of ammonium nitrate, other easily melting solids or in water [5], [6]. The low temperature pyrolysis of the solutions (at about 300°C) produced amorphous precursors, whereas their subsequent annealing at temperatures in the range 500°C–1200°C provided nanocrystalline materials of necessary compositions with the mean dimensions of the grains from 10 nm to 100 nm and greater, which could be regulated by variations in annealing temperatures and durations [2].This method provides wide opportunities for doping of scintillating materials with many light emission activators and other useful ions. It is important to emphasize that several doping elements can be introduced simultaneously by means of thermally induced diffusion.The dimensions of the grains were found from half-width of X-Ray diffraction reflections, by transmission and scanning electron microscopy. A D500 Siemens X-Ray diffractometer, a JEM-100CX transmission electron microscopy and a SUPRA 50VP spectrometer were used for these purposes correspondingly. The SUPRA 50VP spectrometer was used simultaneously with scanning electron microscopy to determine chemical compositions of nanoparticles by analyzing their X-Ray characteristic spectra (i.e., electron microprobe analysis). The crystal structures were found using X-Ray diffraction spectra obtained by means of the D500 diffractometer.Light emission characteristics of the materials were measured by means of optical spectrometers using either X-Ray or optical excitations (continuous and pulsed).Atomic compositions of the materials were found by means of infrared vibration spectroscopy on an IFS—113 "BRUKER" Fourier spectrometer.

III. Experimental Results

Transmission electron microscopic images of lutetium fluoride and lutetium borate particles are shown in Fig. 1 (top and bottom right photos). The bottom left picture presents scanning electron microscopic image of lutetium fluoride microparticles

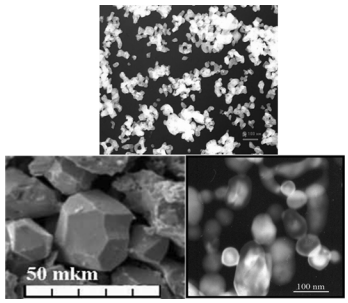

Fig. 1. Transmission electron microscopic images of nanoparticles of lutetium fluoride (top) and lutetium borate (bottom right). Scanning electron microscopic image of lutetium fluoride microparticles (bottom left).

TABLE I
Dependence of Average Diameters of Lutetium Borate Grains on Annealing Temperature

Temperature	500°C	700°C	800°C	1000°C
Diameter	10 nm	30 nm	70 nm	100 nm

for illustration of the changes in sizes and morphology of the particles during annealing (the crystallographic faces are seen quite clearly). It has been found that dependences of the dimensions, morphologies and light emission abilities of lutetium borate and lutetium fluoride particles have significant differences.The $LuBO_3$ nanocrystals demonstrated smooth surface without sharp corners (see Fig. 1) and their geometry was close to spherical. Average diameters of these particles were growing monotonously with the increase of annealing temperature.The typical dependence of average diameters of lutetium borate nanoparticles on annealing temperatures is presented in Table I. Duration of each annealing was about 4 hours.

Behavior of dimensions and morphology of LuF_3 particles, as functions of the annealing temperature, was much more complicated. X-Ray diffractometry revealed significant anisotropy of their dimensions: in the temperature range from 350 to 1000°C the particles were flat. For example, after annealing at 750°C they had 35-nm thickness in [1] direction, and about 70-nm thickness in perpendicular and transverse directions, [100] and [010]. On the other hand, the transmission electron microscopy of these particles (Fig. 1) showed presence of sharp corners and quasi-plane faces even for particles of relatively small dimensions (about 30 nm). Scanning electron microscopy of lutetium fluoride particles with much greater microscopic dimensions (bottom left at Fig. 1) demonstrated preservation of the faceted structure with sharp corners and pronounced crystallographic anisotropy of faces. But the mean dimensions along different crystallographic directions became closer to each other.The dimensional dependence of integral luminescence intensity of lutetium borate particles doped with cerium looks similar to the dependence of YAG:Eu described earlier [2]. It has a light emission pronounced maximum corresponding to the mean diameter of about 90 nm (Fig. 2). The integral luminescence intensity of LuF_3 nanoparticles demonstrated essential changes as the annealing function, but the character of these changes differed strongly from those of $LuBO_3$. After the initial stage of nucleation of these nanoparticles by thermal decomposition of the solution at 350°C, the

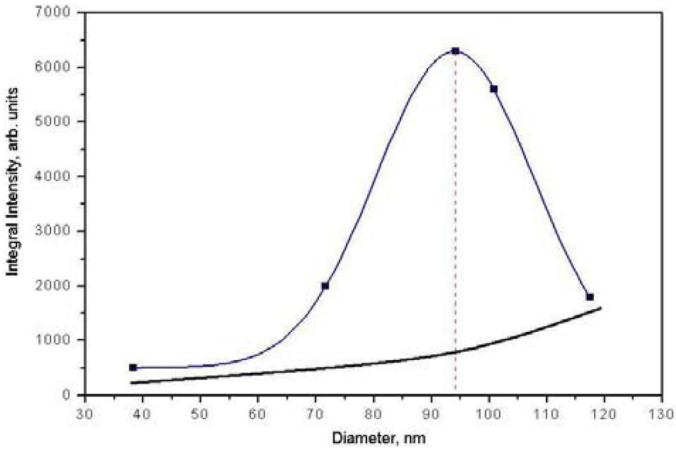

Fig. 2. Dependences of integral intensities of X-Ray luminescence of lutetium borate (the curve with maximum) and lutetium fluoride (monotonous curve) on average sizes of the particles.

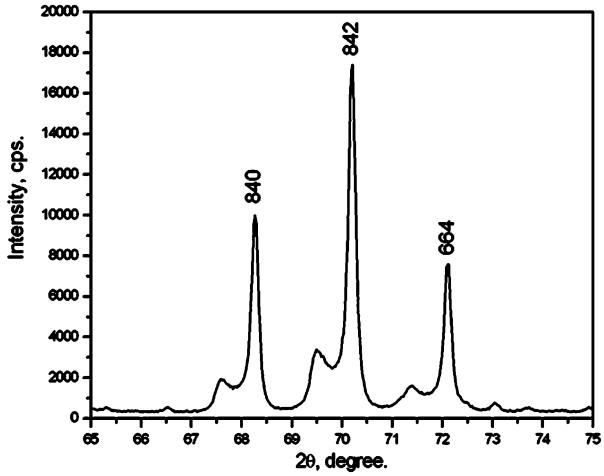

Fig. 3. X-Ray diffractogram of lutetium borate nanoparticles demonstrating the existence of two interatomic spacings.

intensity was relatively weak. The structure of the material was a mixture of amorphous and crystalline states (as X-Ray diffractometry showed). There was 1.5–2-fold increase in emission intensity after the first hour of annealing at 500°C. The structure became crystalline simultaneously. But further annealing at this temperature again caused decrease in the intensity. During subsequent annealing at higher temperatures, either the dimensions or the light emission intensity were growing monotonously. This is shown schematically in Fig. 2. We should note that the curve corresponding to lutetium fluoride is presented for demonstration of qualitative difference in behavior of lutetium borate and fluoride and cannot be used for quantitative conclusions. One of the reasons is that the particles are flat plate-shaped and their sizes in [001] and [100] directions differ by about 2 times. X-Ray diffractometry (for oxide nanoparticles) and infrared spectroscopy for lutetium fluoride particles distinctly revealed non-homogeneities of their crystalline structures for the nanoparticle sizes from 20 nm to 100 nm. Fig. 3 presents a part of X-Ray diffractogram of lutetium borate nanoparticles where splitting of the reflections is seen clearly. Secondary maxima at left of the main maximum reveal the presence of an additional phase with similar symmetry and slightly increased (about 1%) interatomic spacing. It should be noted that splitting of the X-Ray reflections for oxide nanoparticles is rather universal phenomenon which was observed for a wide set of simple rare earth oxides (Lu_2O_3, Gd_2O_3, Eu_2O_3 , La_2O_3) as well as for complex oxides ($LuBO_3$—lutetium borate, $Y_3Ga_5O_{12}$—yttrium-gallium garnet, $Eu_2(MoO_4)_3$—europium molibdate) [6]. The angular widths and intensities of the secondary maxima at lower angles are strongly dependent on the history of particles (temperatures and durations of annealing, degree of mechanical processing by ball milling, etc.). E.g., these additional reflections appeared after moderate duration of annealing (for yttrium-gallium garnet it took 6 hours at 1250°C), but after longer annealing at the same temperature (25 hours for YGG) they disappeared. For lutetium borate and europium molibdate the secondary reflections were observed especially clearly after several hours of ball milling. It is important to emphasize that stoichiometry either of the single-phased or two-phased particles was the same with the accuracy of 1.0% as it was found by electron microprobe analysis. X-Ray diffractometry of LuF_3 did not reveal additional separate reflections, but these reflections were broadened and the temperature dependence of this broadening was rather complicated. At the initial stage of annealing the reflections had triangular-like shapes and broadening appeared either at lower or higher diffraction angles [6]. This behavior of the diffraction pattern can be interpreted as a result of gradual changes in the interatomic spacings in both directions with respect to the bulk material. I.e. regions either with increased or decreased interatomic spacing were presented. Further annealing caused deformations of the reflections, in particular, in high angular region the bulk material spectrum is approached, whereas at lower angles the broadening was preserved. Thus we concluded that at this stage the lutetium borate particles were transformed to the structure with gradual increase of the lattice parameter from the centers of the particles to their exterior surfaces [6]. On the other hand, infrared reflection spectroscopy of these particles after 500°C annealing showed the presence of a new material—lutetium fluoride-oxide $LuO_{1-x}F_{1+2x}$ (Fig. 4). These modifications of the infrared spectra were observed for the lutetium fluoride particles described above, which at the beginning of 500°C annealing increased their light emission ability, but after several hours of annealing at this temperature the luminescence intensity decreased.After processing of lutetium fluoride particles in fluorine containing medium their light emission ability was enhanced and infrared reflection spectrum returned to that of "pure" LuF_3.

IV. Discussion of the Results

The special features of X-Ray diffractograms of oxide nanoparticles and infrared spectra of lutetium fluoride can be attributed to the presence of subsurface layers whose atomic structures differ from the volume structures. It is easier to interprete the nature of this layer in lutetium fluoride where $LuO_{1-x}F_{1+2x}$ phase was found. Fluorine ions are substituted by oxygen ions in oxygen containing atmosphere. At the beginning of this process oxygen-containing regions do not cover the

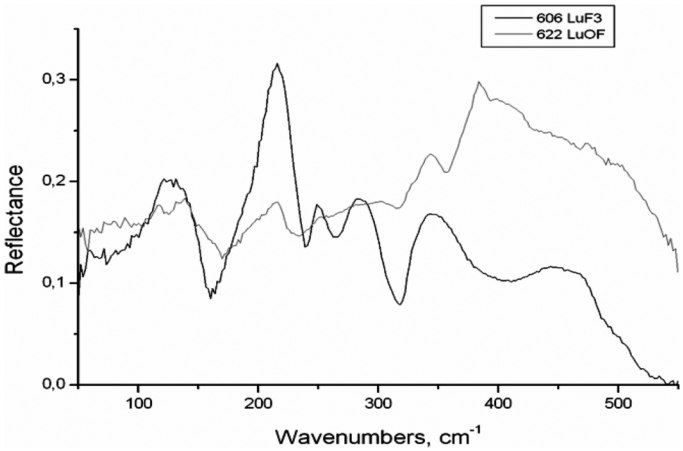

Fig. 4. Infrared reflection spectra of lutetium fluoride (thick curve) and lutetium oxide—fluoride (thin curve).

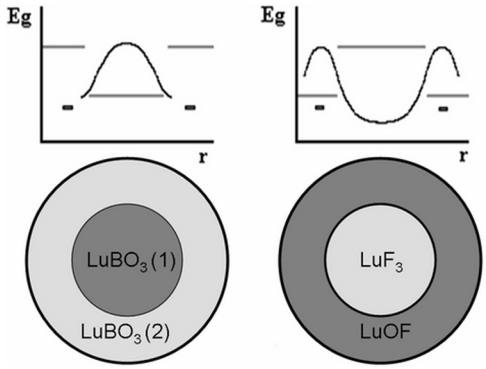

Fig. 5. Schemes of energy and electron structures of lutetium borate (left) and lutetium fluoride (right) nanoparticles. The curves show qualitatively spatial distributions of the electron excitation densities. The drawings at the bottom show schematically spatial distributions of the forbidden gaps (light—wider, dark—narrower).

whole particle surface with a continuous layer. At this moment the influence of oxygen on the infrared reflection spectra and the light emission intensity is relatively weak. On the other hand, the crystalline structure became more regular and the enhancement of the luminescence was observed. Increase in the annealing duration caused an increase in the oxygen content in the subsurface layer thus making light emission decrease and $\mathrm{LuO}_{1-x}\mathrm{F}_{1+2x}$ spectrum manifest. Heat treatment of fluorine-containing medium produced inverse substitution of oxygen by fluorine, which caused recovering of the light emission ability and restoration of the infrared spectra of initial lutetium fluoride.Interpretation of splitting of X-Ray reflections of lutetium borate particles is not so simple. Presence of the secondary maxima adjacent to the main maxima from the left reveals the existence of a new phase with a similar symmetry and slightly increased interatomic spacings (by about 1% as it was stated earlier). But justification of the presence of this new phase in the form of a subsurface layer needs additional argumentation. An alternative version includes existence of a secondary phase, either as inclusions in the matrix particles or as separate particles with increased interatomic spacings. Growth of separate particles with changed lattice parameters can result from variation in stoichiometry of the material. But electron microprobe analysis did not reveal any modification in the stoichiometry even for the particles with the integral intensity of the secondary reflections at the level of 30%. So, existence of the secondary phase as separate particles is doubtful. On the other hand, the increase in volume fraction of these secondary phases after mechanical processing of oxide particles by ball milling draws to the assumption that these phases are concentrated mainly in the subsurface layers of the particles. This version is confirmed by well known idea that the internal energy of the subsurface layer is higher than in the volume, so its structure can be more similar to the high temperature state of the material with increased interatomic spacings [7]. One more argument in favor of the secondary phases localization in the subsurface layers of the particles is that the contents of these phases estimated independently from the integral intensities of the secondary X-Ray reflections and from the widths of the additional maxima agree. For the diffractogram presented in Fig. 3 both approaches gave the values of about 30% (the thickness of the secondary phase layer estimated from the width of the secondary reflections is about 10% of a particle radius). It should be emphasized that the ratio between the secondary phase thickness in the subsurface layers and the overall diameter of the particles is not constant. It is significantly dependent on chemical compositions, overall dimensions and the way of the treatment of the particles. In our experiments we observed the thicknesses from 2 nm to 20 nm or even more.The existence of the subsurface layers with the increased interatomic distances (as in oxides) or with oxygen containing phases (as in fluorides) is used to explain at least three experimental results described above: presence of the maximum light emission effectiveness as a function of diameters of oxide nanoparticles, its absence for fluoride particles and essential acceleration of the scintillation rise time for oxide nanoparticles.In the rare earth metal oxides, in accordance with the ion model of interatomic binding (see, for example, [8]), the increase in interatomic spacing leads to corresponding increase in the forbidden gap of a material. Substitution of fluorine ions by oxygen in lutetium fluoride should induce the contrary effect—a. decrease in the forbidden gap width. So the influence of the subsurface layers on the processes of electron excitation recombination in the oxide and fluoride nanoscintillators is quite different (see the scheme at Fig. 5). In oxides like lutetium borate, yttrium-aluminum garnet, and others the subsurface layer with the increased gap width protects the excitations from direct contact with the surface. It is well known that usually the surface provides many channels of non-radiative recombination, so this protection is important for increase in the light emission ability. On the other hand, the decreased gap at the subsurface layer of lutetium fluoride attracts excitations to the surface and consequently enhances their non-radiative recombination. Due to this reason the light yield in lutetium fluoride is increasing gradually with the increase in diameter of the particles, because the bigger the diameter, the lower the probability of electron excitation contacts with the surface.There can be several reasons why these maxima of the light emission ability appear to be functions of the nanooxide particles sizes. For example, at 70–100-nm diameters when

these maxima are observed, the exterior perimeters of the particles are roughly close to the emitted light wavelength (taking into consideration that the refraction index is about 2). So, the nanoparticles can work as optical resonators for the emitted photons. It is well known that in this case [1] the probability of spontaneous light emission is increased as the density of the virtual photons in the resonator increase in proportion to the resonator quality and inverse proportion to its volume and to power of three of the emitted light wavelength (the so called "Purcell effect"). In our case the volume of the particles is close to cube of the wavelength, so for good quality of the resonator (i.e., for smooth enough external surfaces of the particles) the enhancement of the light emission due to Purcell effect should be rather strong. This is the case for approximately spherical particles of lutetium borate and yttrium-aluminum garnet. But for lutetium fluoride particles the quality of the resonator is poor because of an substantial fraction of sharp corners and edges, which scatter the emitted light effectively. On the other hand, the presence of the subsurface layer (of the thickness from 2 to 20 nm) with modified atomic and electron parameters can provide conditions for effects of quantum confinement of electron and phonon states, whereas the overall dimensions of the particles are far from this condition.The close contact between two dielectric regions with different positions of valence bands provides the so called double layer which is electrically active due to migration of a certain amount of charge carriers from one region to another. Due to this migration quasi-two dimensional region with increased electrostatic field should appear. It is quite possible that this region has nanoscopic thickness, so the conditions for quantum confinement can also exist in this case.Hence, the complicated layered structure of the oxide nanoparticles provides several reasons for various quantum effects, which can cause enhancement of the light emission ability. Clarification of these mechanisms needs more detailed studies, which we plan to arrange later.The same layered structure can be applied for explanation of the rise time acceleration of the light emission observed in the lutetium and gadolinium borate nanoparticles. E.g., due to electrical activity of the double layer described above two phenomena can take place: electron-hole pairs will be attracted to this layer as well as the ions which work as light emission activators (they are shown as bright points in Fig. 5). The subsurface layer is also attractive for doping with various ions for thermodynamic reasons: the subsurface layer being a region of higher internal energy is more advantageous for impurities introduction than the interior volume.Thus, due to the abovementioned reasons both concentrations (of electron-hole pairs and of light emission centers) can be increased significantly in the subsurface layer. This will cause increase in the frequency of collisions of electron excitations with the emission centers and consequent increase in the capturing rate of these excitations by the activators. So the centers will be saturated with electron excitations much faster than in a homogeneous region. Thus the rise time of the light emission will be decreased substantially.In addition, we would like to emphasize that in polymorphic materials (which can have several phases) the layered structure can be formed from the regions containing different phases, as we have observed in europium molibdate [9].Generally speaking, capture of non-equilibrium electrons and holes excited by light emission activators inside non-metal nanoparticles should be accelerated in any case when these activators are concentrated in the subsurface layer. Due to internal reflections at the surfaces of nanoparticles, electron excitations will spend more time in the vicinity of the surface than in the volume. So the frequency of electron and hole collisions with the activators will be increased, as the time required for filling the centers with electron excitations will be decreased.Non-metal particles with nanoscopic dimensions provide a wide set of opportunities for ionizing radiation registering with temporal resolution better than 1 ps (i.e., 10^{-12} seconds). For example, relaxation of a pair of hot electron and deep hole produced by photoelectric absorption of X-Ray quantum by any atom will proceed much faster (during the time less than 1 ps) if this atom is in contact with other atoms in a cluster or a nanoparticle. In this case the energy of the absorbed quantum will be dissipated due to emission of secondary X-Rays and Auger electrons by the neighbors of the atom which was the absorber of the initial quantum (see [10] and references there) and this dissipation will be far shorter than 1 ps. The rest part of the absorbed energy will be transferred to the phonon system of a nanoparticle faster than for 1 ps. Due to relatively small dimensions of the absorbing nanoparticle, which is isolated form the neighboring particles by the exterior surface, emission of Auger electrons as well as transfer of the rest part of the absorbed quantum energy to the phonon system of the particle should induce noticeable changes in its physical properties. E.g., emission of the electrons to the exterior space will induce local dipole moments and electric fields, which can be detected by optical or other means. On the other hand, significant perturbations of internal crystal fields or atomic vibrations can induce structural transformations in nanoparticles of the polymorphic materials—like vanadium oxide [11] or europium molibdate [7]. Experimental studies of structural transformations in VO_2 showed that in the nanosized objects these transformations can proceed faster than for 1 ps [11]. They will induce respectively fast changes in optical characteristics of the particles.The techniques for registration of these fast modifications of local optical characteristics with femtosecond lasers are well developed [10], [11]. So the prospect of development of a radiation detector with sub-picosecond temporal resolution with application of nanoparticles seems realistic.Superfast radiation detectors will have promising prospects for applications among new generations of X-Ray devices for medical diagnostics, security control, etc. For example, time-of-flight registration with 1 ps temporal resolution provides 3-dimensional X-Ray imaging of various interior objects with spatial depth resolution of about 0.3 mm. So volume imaging for medical testing will not need tomographic angular scanning. Hence, irradiation doses for the patients will be decreased significantly and the diagnostic procedures will be accelerated. Both these factors are important for improvement of medical diagnostic.Nano-dimensions of radiation detectors give good opportunities for development of detectors with much higher radiation hardness. These opportunities are based on the attraction of any structural defects induced by irradiation to the exterior surface, because these defects inevitably increase the internal energy. In nanoparticles a probability for the de-

fects to achieve the surface by diffusion and annihilate there is very high because of very short distances from any internal point to the surface. The characteristic time of the diffusion is proportional to the ratio of the square distance to the diffusion coefficient [12]. For nanoparticles having the radius about 20 nm and typical diffusion coefficient of 10^{-14} $\mathrm{cm}^2/\mathrm{sec}$ the annihilation time thus estimated will be about 100 seconds. This means that after absorption of X-Ray or gamma quanta the nanoparticles will recover after 100 seconds. The density of nanoparticles of these sizes (i.e., their number per 1 cm^3) is of an order of 10^{17} cm^{-3}. So the effective absorption layer of 0.1-mm thickness will contain 10^{15} nanoparticles per cm^2 of its area. If each nanoparticle needs 100 seconds for recovery after gamma or X-Ray absorption, the flow intensity of these quanta which will not destroy the stability of the nanoparticles can be estimated as $10^{13}/n\ \mathrm{cm}^{-2}\ \mathrm{sec}^{-1}$. Here n is the total number of the nanoparticles disturbed by secondary X-Rays and electrons emitted during relaxation of the particle, which absorbed the first quantum [9]. Precise estimations of this quantity is problematic and needs additional experiments, but if this value does not exceed 100 particles, then the acceptable irradiation flow can achieve $10^{11}\ \mathrm{cm}^{-2}\ \mathrm{sec}^{-1}$. This flow of ionizing radiation is close to typical values inside nuclear reactors [13]. Hence, nanoscintillators can be used for development of radiation detectors with increased radiation hardness, which can survive in the flow of intensive radiation. Moreover, the upper limit of the radiation flow can be increased significantly by decrease in dimensions of the nanoscintillators, because this limit is inversely proportional to the square of the dimensions. On the other hand, slight increase in temperature of the detector exploitation will cause several-fold increase in the self-diffusion coefficient, which will provide the corresponding increase in radiation hardness of the nanoscintillators.Excellent prospects of application of nanoparticles for radiation detectors described above have one severe obstacle. It is caused by difficulties in preparation of optically transparent bulk material from nanoparticles. High temperature compaction usually applied for this purpose will increase the dimensions of the particles, so the advantages provided by nanodimensions will be lost. So, new methods for practical application of nanocrystalline radiation detectors should be developed. For example, thin layer of nanoparticles can be deposited onto optically transparent light guide. This opportunity is especially important for the development of radiation hard detectors for on-line control of nuclear reactors. We should note that production of light guides from sapphire fibers (including the fibers with radiation hardness up to 10^6 Grey) is well developed [14], [15].

V. Conclusion

The experiments and arguments presented in this paper show that application of nanocrystalline scintillators for radiation detectors can improve their parameters significantly; achieve manifold increase in the light yield and sensitivity; accelerate the registration rate of ionizing radiation to the temporal resolution better than 1 ps; provide new possibilities for X-Ray volume imaging by using time-of-flight registration, reducing irradiation doses, duration of scanning and cost of devices; and increase essentially radiation hardness of the detectors (which is important for radiation monitoring at nuclear power plants, etc.)

References

[1] J. P. Reithmaier *et al.*, "Strong coupling in a single quantum dot—semiconductor microcavity system," *Nature*, vol. 432, pp. 197–197, 2004.

[2] N. V. Klassen, I. M. Smyt'ko, G. K. Strukova, V. V. Kedrov, N. P. Kobelev, E. A. Kudrenko, A. P. Kiseliov, and N. F. Prokopiuk, A. Gektin and B. Grinyov, Eds., "Improvement of scintillation parameters in complex oxides by formation of nanocrystalline structures," in *Proc. 8th Int. SCINT Conf.*, Crimea, Ukraine, Sep. 2005, pp. 228–231.

[3] J. Wilkinson, K. B. Ucer, and R. T. Williams, "The oscillator strength of extended exciton states and possibility for very fast scintillators," *Nucl. Instrum. Methods Phys. Res. A*, vol. A537, pp. 66–70, 2005.

[4] E. I. Rashba and G. E. Gurgenishvili, "To the theory of the absorption edge in semiconductors," *Sov. Phys.—Solid State*, vol. 4, pp. 759–805, 1962.

[5] N. V. Klassen, S. Z. Shmurak, I. M. Shmyt'ko, G. K. Strukova, S. E. Derenzo, and M. J. Weber, "Structure and luminescence spectra of lutetium and yttrium borates synthesized from ammonium nitrate melt," *Nucl. Instrum. Methods Phys. Res. A*, vol. A537, pp. 144–148, 2005.

[6] I. M. Shmytko, E. A. Kudrenko, G. K. Strukova, V. V. Kedrov, and N. V. Klassen, "Anomalous structure of nano-crystallites of rare earth compounds received by sol-gel methods," in *Proc. Abstracts Int. Conf. Size-Strain V, Difraction Analysis of the Microstructure of Materials*, Garmisch-Partenkirchen, Germany, Oct. 2007, pp. 115–116.

[7] G. M. Sergeev, *Nanochemistry*. Amsterdam, The Netherlands: Elsevier, 2006.

[8] J. M. Ziman, *Principles of the Theory of Solids*. Cambridge, U.K.: Cambridge Univ. Press, 1964.

[9] S. Z. Shmurak, I. M. Shmyt'ko, V. V. Sinitsyn, B. S. Red'kin, A. P. Kiseliov, N. V. KLassen, E. A. Kudrenko, and N. F. Prokopiuk, A. Gektin and B. Grinyov, Eds., "Correlation of light emission properties of rare earth molibdates with modifications of their structure," in *Proc. 8th Int. SCINT Conf.*, Crimea, Ukraine, Sep. 2005, pp. 121–124.

[10] A. I. Kuleff and L. S. Cederbaum, "Tracing ultrafast interatomic electronic decay processes in real time and space," *Phys. Rev. Lett.*, vol. 98, pp. 08301–08301, 2007.

[11] A. Cavalleri, C. Toth, S. W. Siders, J. A. Squier, F. Raksi, P. Forget, and J. C. Kieffer, "Femtosecond structural dynamics in during an ultrafast solid—Solid phase transitions," *Phys. Rev. Lett.*, vol. 87, no. 23, pp. 237401-1–237401-4, 2001.

[12] W. F. Smith, *Foundations of Materials Science and Engineering*, 3-D ed. New York: McGraw-Hill, 2004.

[13] B. T. Price, C. C. Horton, and K. T. Spinney, *Radiation Shielding*. New York: Pergamon, 1957.

[14] P. I. Antonov and V. N. Kurlov, "A review of developments in shaped crystals growth of sapphireby the stepanov and related techniques," *Prog. Cryst. Growth Charact. Mater.*, vol. 44, pp. 63–122, 2002.

[15] J. J. Fitzgibbon and J. M. Collins, "High volume production of low loss sapphire optical fibers by saphikon efg (Edge defined, film-fed Growth) method," *Proc. SPIE*, vol. 3262, pp. 135–141, Jan. 1998.